

# Cooling of Shielding with Pressurized Helium Gas

Bob Weggel 10/19/2011

Using MARS, Nicholas Souchlas has predicted the energy-deposition density in numerous target magnets, especially geometry “IDS120h,” shielded by various percentages of tungsten-carbide or tungsten, cooled by water or helium, in vessels of stainless steel or tungsten. Fig. 1 shows two illustrative histograms. Each includes a region with a heating density on the order of 10 W/g, or 200 W/cm<sup>3</sup>.

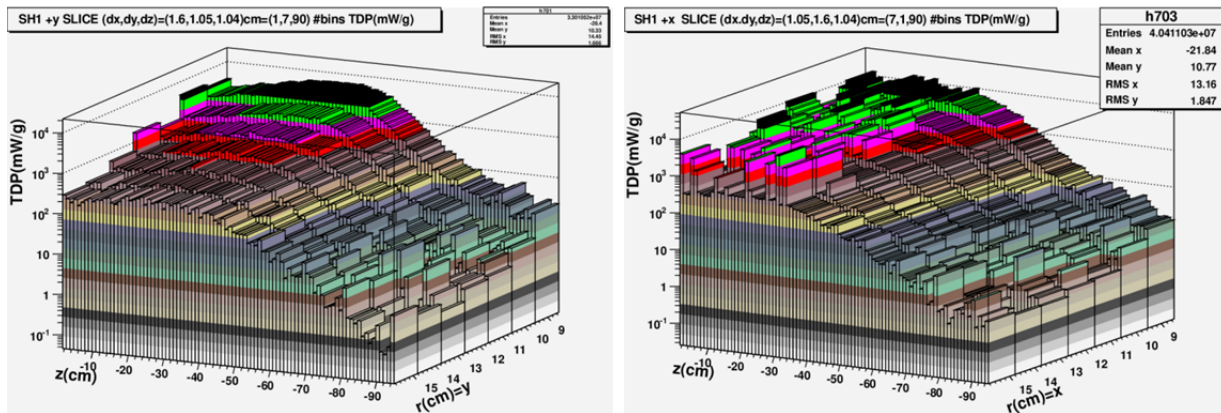
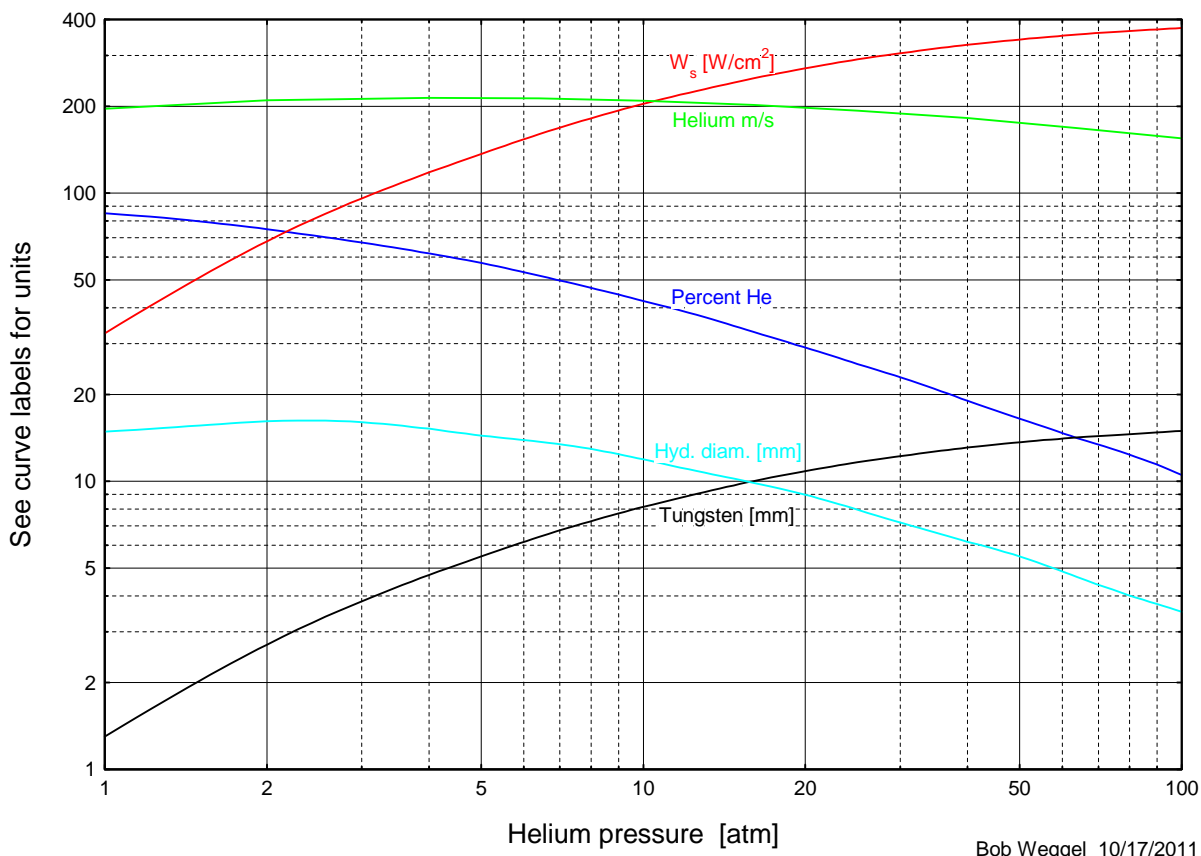


Fig. 1a & b: Histograms of energy-deposition density in shielding. Left: Plane of magnet axis (z) and vertical axis (y). The region of greatest heating (black or green) extends only 2 cm in y but nearly 50 cm in z. Right: Horizontal, (x, z), plane, with heating that is more diffuse (~5 cm in x) and has greater statistical bin-to-bin scatter.

The histogram bin for  $\langle x \rangle = 9.0$  cm,  $\langle z \rangle = -16.6$  cm has an energy-deposition density of 14 W/g, or  $\sim 270$  W/cm<sup>3</sup> of tungsten. Such a high energy-deposition density is a daunting challenge for cooling with helium gas. A simplified model of cooling, with high-velocity gas sandwiched between a pair of infinitely-wide, thin slabs of shielding, predicts that with helium at atmospheric pressure and an inlet-to-exit pressure drop of 10% (0.1 atm), one must allocate 85%(!) of the shielding volume to coolant channels, given the following parameters: 1) helium velocity  $\approx 200$  m/s; 2) tungsten temperature rise = 80 °C; 3) uniform heating density  $W_v$  of 250 W/cm<sup>3</sup>; 4) slab extent in direction of coolant flow = 5 cm, as suggested by Fig. 1b; and 5) heat conduction only perpendicular to the cooled surface.

In a system optimized to minimize the shielding volume lost to coolant, the optimum hydraulic depth—twice the depth of the channel if it is very wide—is 15 mm, if the coolant-passage length is one meter. The thickness of tungsten that is cooled is only 1.3 mm, in order to limit the heat-flux density  $W_s$  to the 33 W/cm<sup>2</sup> given by the product of the boundary-layer temperature differential  $\Delta T_{bl}$  of 53 °C and the heat-transfer coefficient  $h$  of only 0.6 W/cm<sup>2</sup>·K. The temperature rise in the bulk of the helium is 27 °C. The gradient temperature rise in the tungsten is negligible, because the tungsten is very thin and conducts heat well—nearly half as well as copper. The coolant channels need a combined cross-sectional area of  $\sim 0.6$  m<sup>2</sup> to remove the  $\sim 2.5$  MW predicted to be deposited in the shielding. This does not include the considerable additional cross section likely to be “wasted” in headers or channels that absorb less heat than allowed by the total temperature rise.

## Parameters of Pressurized-Helium-Cooled Tungsten with $250 \text{ W/cm}^3$ Heating



Bob Weggel 10/17/2011

Fig. 2. Selected cooling parameters of Target Magnet “IDS120h” vs. average pressure of helium-gas coolant. Inlet-to-exit pressure drop is 10% of average pressure.

As shown in Fig. 2, one can improve the cooling greatly by raising the helium pressure to well above one atmosphere. Increasing the helium pressure and pressure drop by an order of magnitude each, to 10 atm and 1 atm respectively, decreases the needed coolant fraction by a factor of two, to ~42%. The pumping power increases by a factor of 86, because the pressure drop and flow rate are greater by factors of 10 and 8.6, respectively. The hydraulic diameter decreases 20%, to 12 mm; the allowable tungsten thickness increases by a factor of six, to 8.2 mm. The boundary-layer, bulk and gradient temperature rises are 60 °C, 20 °C and 0.5 °C, respectively. The cross section needed for 2.5 MW of cooling decreases by a factor of 8, to  $0.07 \text{ m}^2$ .

Increasing the helium pressure and pressure drop by another factor of ten—to 100 atm and 10 atm, respectively—decreases the needed coolant fraction by a factor of four, to 10.5%. The pumping power increases by a factor of 22, because the pressure drop and flow rate are greater by factors of 10 and 2.2, respectively. The hydraulic diameter decreases to 3.6 mm, 30% of the value at 10 atm. The allowable tungsten thickness increases 83%, to 15 mm. The boundary-layer, bulk and gradient temperature rises are 61 °C, 17 °C and 1.6 °C, respectively, little changed from the values at 10 atm. The cross section for 2.5 MW of cooling decreases by a factor of six, to  $0.012 \text{ m}^2$ .

Even for water, a heating density of  $250 \text{ W/cm}^3$  is challenging. Water at a pressure drop of 10 atm can cope with cooling requirements that are much more demanding—e.g., cooling the shielding with channels  $\sim 10 \text{ m}$  long that encounter a heated zone  $\sim 50 \text{ cm}$  long (see Fig. 1), parameters appropriate for cooling channels that are axial rather than radial—but to do so requires 24% of the shielding volume be allotted to coolant, and the peak heat flux density is as high as in Bitter magnets.

The analysis leading to Fig. 2 exploited the localization of heating density in at least one of the three directions  $[x, y, z]$  or, more appropriately, given the quasi-cylindrical symmetry,  $[r, \theta, z]$ . The localization limits the bulk temperature rise in the helium. Figure 3 curve-fits heating-density values predicted by Souchlas (file “IDS120h\_TDP\_SLICE\_PEAK\_REGION\_px.txt”) along three radial rays through regions of very high heating. The curve fits reveal that the heating is localized to a region only half the 5-cm size used to generate Fig. 2. For example, to match the maximum height ( $13.4 \text{ W/g}$ ) and integral ( $31.2 \text{ W}\cdot\text{cm/g}$ ) of the red curve of Fig. 3, a square-wave function would need a width of only 2.3 cm.

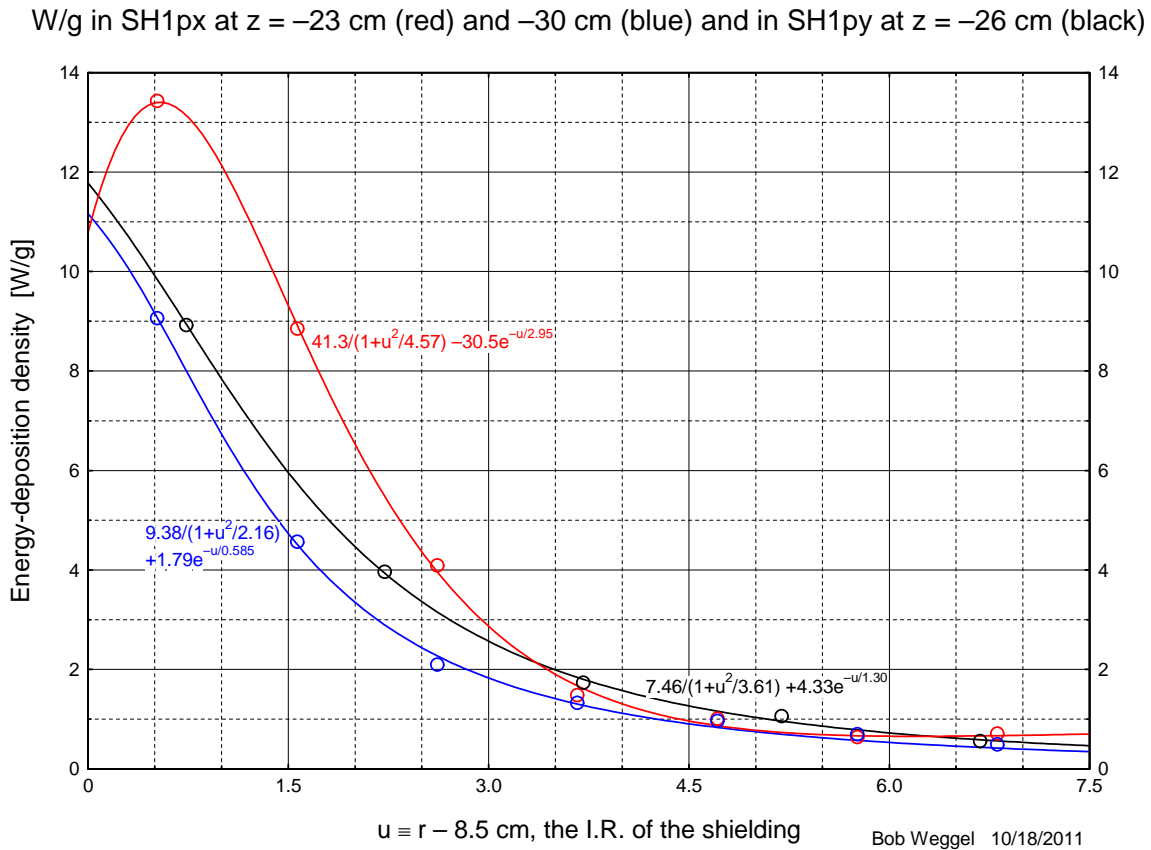


Fig. 3: Energy-deposition density  $W_v(u)$ , where  $u \equiv r - r_0$ , and  $r_0 = 8.5 \text{ cm}$ , the I.R. of the shielding. Red points ( $z = -23 \text{ cm}$ ) are for the radial ray that passes through a region of near-maximum energy-deposition density.

The upper block of Fig. 4 plots the energy-deposition density in tungsten shielding given by the red curve of Fig. 3. The lower block plots the heating density predicted for copper—chosen for its higher thermal conductivity, to improve the cooling of hot spots, and for its reduced heating density, presumed inversely proportional to interaction length—9.6 cm for copper vs. 15.1 cm for tungsten. The respective peak heating densities are  $260 \text{ W/cm}^3$  and  $160 \text{ W/cm}^3$ .

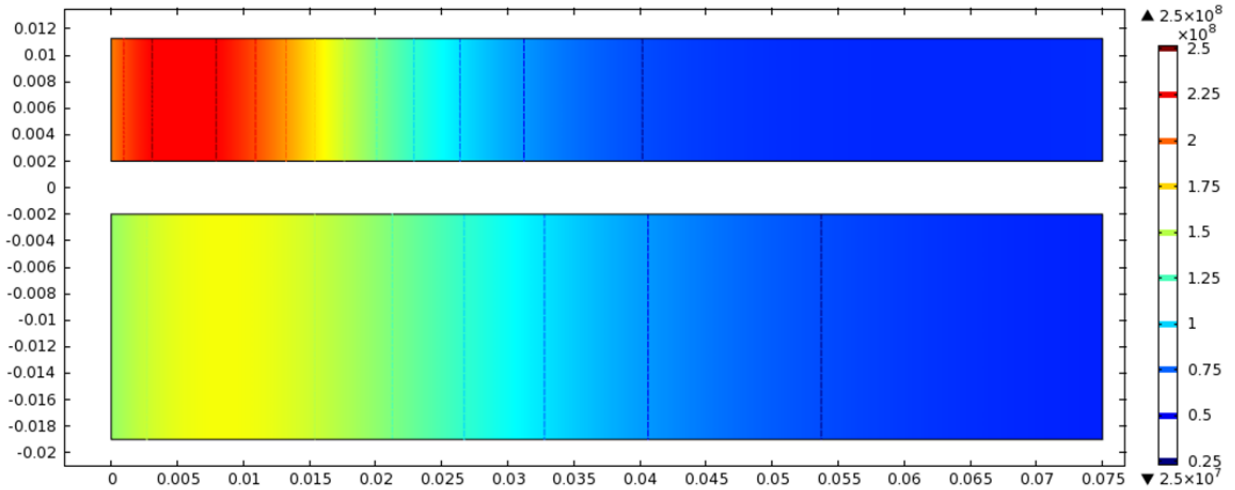


Fig. 4: Energy-deposition density [ $\text{W}/\text{m}^3$ ; divide by  $10^6$  to get  $\text{W}/\text{cm}^3$ ] in slabs of tungsten (upper rectangle) or copper (lower rectangle). Dimensions are in meters.

Fig. 5 shows the temperature (colors and contours) and heat-flow direction (arrows) in the slabs of Fig. 4 when cooled on the left-hand face and one of the two broad faces—upper face of tungsten; lower face of copper—by 10-atm helium at 210 m/s (Dittus-Boelter heat-transfer coefficient:  $h = 3.4 \text{ W}/\text{cm}^2 \cdot \text{K}$ ). The thickness of each slab—9.3 mm for tungsten, 17 mm for copper—is the maximum allowed by the 80-C limit on peak temperature rise. These thicknesses are greater by 14% and 38%, for tungsten and copper respectively, than predicted with longitudinal conduction ignored. Even so, it will be a challenge to perforate all components with coolant passages sufficiently closely spaced to keep the heat flux, and therefore the temperature rise, within the desired limits.

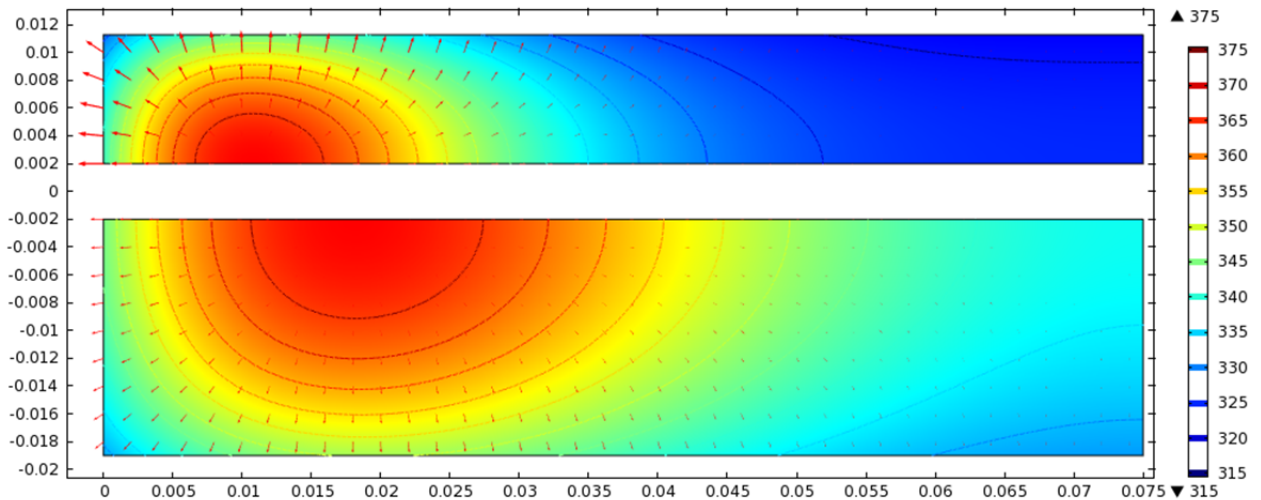


Fig. 5: Temperature (colors and contours) and heat-flow direction (arrows) in tungsten (upper rectangle) or copper (lower rectangle) slabs heated as in Fig. 4 and cooled on one face and left end by 10-atm helium at 210 m/s (heat-transfer coefficient:  $h = 3.4 \text{ W}/\text{cm}^2 \text{ K}$ ). Slab thicknesses are 9.3 mm (tungsten) and 17 mm (copper).